

FEASIBILITY OF FIDUCIAL-FREE PRONE-POSITION TREATMENTS WITH CYBERKNIFE FOR LOWER LUMBAR/SACRAL SPINE LESIONS

Fürweger C^{1,*}, Drexler C¹, Kufeld M¹, Wowra B¹

¹European Cyberknife Center Munich, Germany

ABSTRACT

Objective: For spinal Cyberknife (CK) treatments, prone patient position can yield a dosimetric advantage for posterior lesions, but the target can be subject to respiratory motion. We treated 17 lower lumbar/sacral lesions in prone position using CK fiducial-free Xsight™ spine tracking and analyzed motion data in order to establish an adequate margin concept. **Methods:** The lumbar spine and pelvis were elevated and stabilized to decouple the target from respiration. The tracking region of interest was centered at the lumbar vertebrae L4/L5. Pairs of X-ray images were taken periodically (1.4 per minute) during treatment. Tracking data from two periods of 6 to 15 minutes per treatment were analyzed to assess the extent of breathing-induced motion. **Results:** Stochastic motion in left/right and superior/inferior direction was small, with peak amplitudes of 0.40 ± 0.20 mm and 0.58 ± 0.31 mm. Anterior/posterior spine motion was significantly increased with a peak amplitude of 1.27 ± 0.50 mm, and was positively correlated with a head-down/up tilt of the spine due to breathing. **Conclusions:** Fiducial-free prone treatments of the lower lumbar and sacral spine are feasible using Xsight™ spine tracking and proper immobilization. The residual impact of respiratory motion can be compensated with an additional PTV margin of 3 mm.

INTRODUCTION

Spinal stereotactic radiosurgery is an increasingly adopted technique (1) that relies on highly accurate delivery of large radiation doses to spinal lesions. For this purpose, different image-guidance methods are applied in order to minimize the geometric targeting error. While, initially, fiducial implants were required for image-guidance (2), current technology alternatively uses the skeletal structure of the spine as positional reference (3, 4, 5).

The current CyberKnife version (CK, Accuray Inc., Sunnyvale, CA) has recently been described in a comprehensive review (6). Briefly, it is comprised of a compact linear accelerator mounted on a robotic arm, and a stereoscopic kV imaging system. For image-guided delivery of CK treatments, different software applications are used to identify the target and to correct the robot position with respect to the current target location.

The CK system is capable of precisely delivering treatments consisting of a large number (>100) of non-isocentric, non-coplanar beams from a large solid angle around the patient. However, due to the specifics of the CK configuration, the space below the treatment table cannot be accessed by the linac, which prohibits posterior radiation beams for patients in supine position. As a consequence, treatment of spinal targets in prone position suggests a potential advantage in terms of total dose and dose to specific organs at risk (e.g. bowel) as well as a reduction in monitor units, provided that additional spine motion due to respiration is adequately managed.

Given the available image-guidance modalities, there are two different ways to treat spinal lesions with CK: First, fiducial tracking, which uses radio-opaque markers (such as screws) attached to the spine and is supported by the manufacturer for both prone (additionally using the Synchrony system for compensation of respiratory motion) and supine position (7). Second, fiducial-free Xsight spine tracking (XST), which uses the skeletal structure of the spine as reference, but is not designed to work in combination with the Synchrony system. XST is therefore supported by the manufacturer for supine treatments only (7).

For lesions in the lower lumbar and sacral spine, the CK user is left with two recommended options: Invasive

implantation of fiducials for prone position treatment, or XST in supine position, at the cost of additional dose to the pelvis. However, despite of prone position, respiration-induced movement of the lower lumbar and sacral spine is low in comparison to the upper lumbar or thoracic spine. It can further be reduced by using proper immobilization techniques. We have therefore performed 17 prone-position treatments using CK Xsight spine tracking for targeting the lower lumbar and sacral spine in order to demonstrate the feasibility of this technique. We have analyzed spine motion patterns during treatment to establish and verify an appropriate margin concept.



Figure 1. Prone setup example. A vacuum cushion was used to elevate the pelvis. For treatment, a belt was used for additional stabilization (upper right, grey belt not yet fastened).

METHODS

Xsight Spine Tracking (XST)

The Xsight spine tracking system (8) matches stereoscopic live images of the spinal region of interest (ROI) with synthetic reference images (digitally reconstructed radiographs – DRRs) to determine the position of the spinal

*Corresponding author: christoph.fuerweger@cyber-knife.net

target. The ROI typically includes three to four adjacent vertebrae. Stereoscopic live images are acquired periodically during treatment to continuously update the positional information. This data is utilized to redirect the incident beams to the current location of the spinal target by automatically adapting the position of the robotic arm. For supine treatments, the XST system has been demonstrated to achieve a clinical accuracy of less than 1 mm despite of intrafraction patient motion (9).

Prone Patient Treatments

A prone position helical CT scan was acquired with 1 mm slice thickness for dose planning and calculation of DRRs. Since the CK software prohibits XST tracking for prone

planning CT scans, they were designated as "supine" despite of patient prone position. As a consequence, left/right and anterior/posterior directions of the dataset are reversed. For scanning, the pelvis was elevated and stabilized using a vacuum cushion, pads and a belt for fixation (fig. 1), as needed. In this manner, we aimed to decouple the anatomy to be treated from respiratory motion. An individually optimized position with minimal motion was identified for each patient. The extent of residual motion in the lower lumbar/sacral spine was visually checked by a physician and a physicist immediately before CT scanning. The final patient position was carefully documented in order to correctly reproduce the setup for treatment.

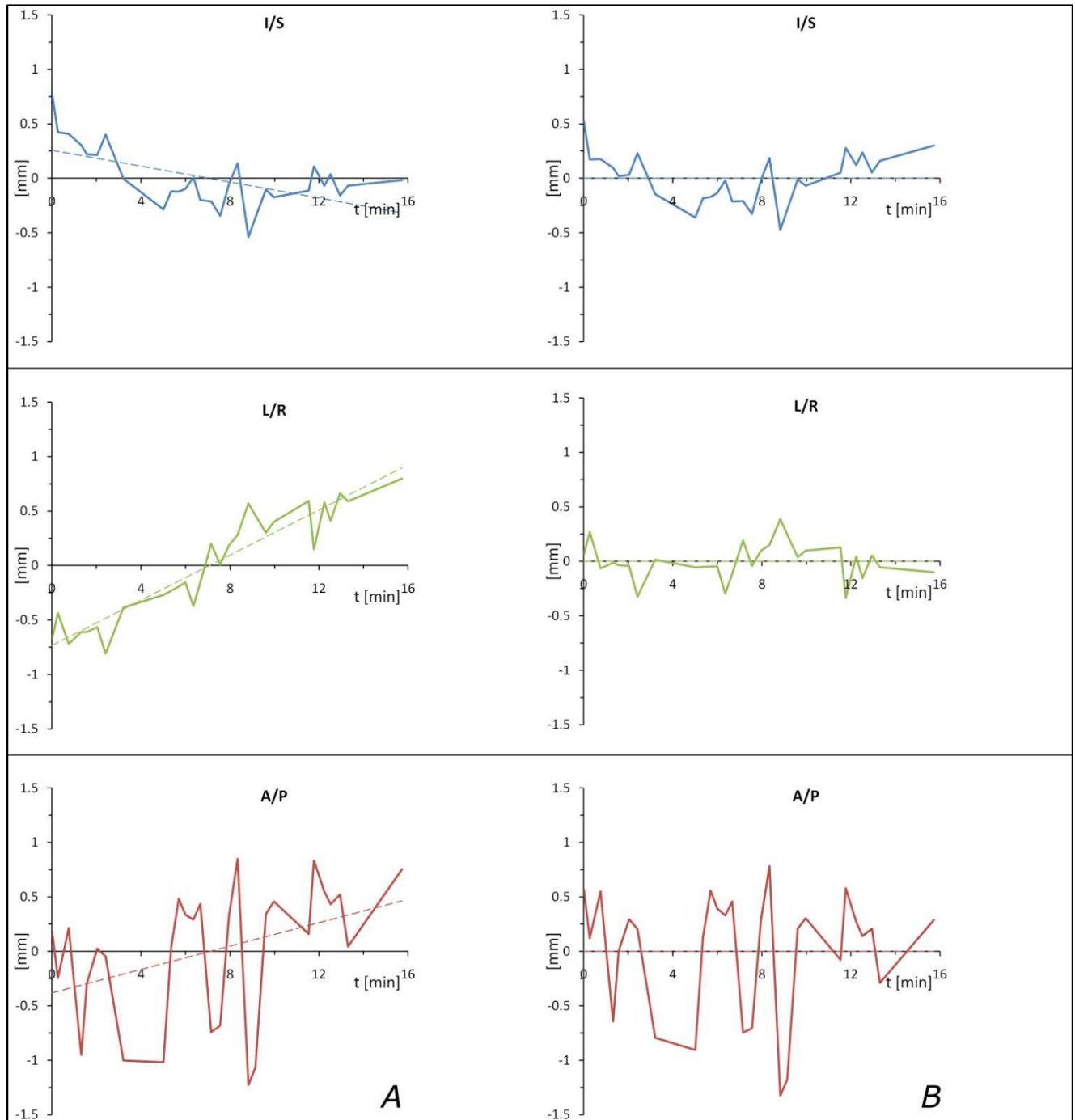


Figure 2. Data analysis for a single observation period of 15 minutes. Translational directions inferior/superior (I/S), left/right (L/R) and anterior/posterior (A/P) are given. A (left): Translational raw data as a function of time. This patient shows a pronounced drift in L/R and comparably minor drifts in I/S and A/P directions, as indicated by least square linear fits. Overall, the extent of systematic drift is above average for this example case. B (right): Stochastic motion as a function of time. By subtracting the drift, the stochastic component is isolated. For this patient, excursions in A/P direction are predominant.

Patients were treated in prone position for a median treatment time of 95 minutes. This timeframe typically included one or two treatment breaks of a few minutes. The tracking ROI was centered at lumbar spine 4/5. For sacral lesions, tracking on the lower lumbar spine has been demonstrated to yield adequate accuracy (10). X-ray images were acquired during treatment every 1 to 3 non-blocked beams. The ROI in each image pair was matched with the corresponding DRRs and the positional deviations were recorded as a 6-dimensional vector with 3 translational (superior/inferior, left/right, anterior/posterior) and 3 rotational components (roll, pitch, yaw).

Data Analysis

We analyzed motion data in all 6 degrees of freedom for 17 single-fraction treatments. For each treatment, two periods of 6 to 15 minutes (mean 13.9) without manual couch repositioning were isolated for analysis of motion patterns (fig.2A). On average, 19 image pairs were acquired during each observation period, which corresponds to a mean image frequency of 1.4 images per minute.

Patient motion patterns are composed of a non-random drift component overlaid by stochastic shifts (11, 12). Since each X-ray acquisition represents a “snap-shot” of a random phase in the breathing cycle, the respiration-induced target motion is included in the stochastic component. We therefore separated and subtracted the target drift in order to assess the extent of breathing-induced motion, using the following simplified formalism: For each observation period, the drift component can be described by a least square linear fit of the positional data as a first-order approximation (fig. 2A). This drift was quantified and subtracted from the raw data to isolate the stochastic part (fig. 2B). The peak amplitude A of the stochastic component (n data points) for translation x was calculated according to

$$A = \frac{\max(x_1..x_n) - \min(x_1..x_n)}{2} \quad (1)$$

By this definition, A includes both respiration-induced positional shifts as well as truly stochastic motion. When the respiratory component is predominant this value represents a measure for the extent of breathing-induced residual motion in a specific direction.

RESULTS

All patients tolerated treatments in prone position reasonably well. By allowing for treatment breaks upon request, all patients were able to maintain this position despite of prolonged treatment times. Xsight spine tracking could be performed with no indication of a regional mismatch.

The mean stochastic motion in left/right and superior/inferior direction was small, with peak amplitudes of 0.40 ± 0.20 mm (median: 0.46 mm) and 0.58 ± 0.31 mm (median: 0.50 mm), respectively (fig. 3). The major contribution to overall stochastic motion was from the anterior/posterior direction, where significantly increased shifts with a mean peak amplitude of 1.27 ± 0.50 mm (median: 1.21 mm) were observed (fig. 3). The extent of anterior/posterior motion was subject to a large patient-specific variation, with a minimum value of 0.38 mm and a maximum of 2.29 mm.

Anterior/posterior stochastic motion was positively correlated with a head-down/up tilt of the spine in 15 out of 17 cases, with a mean rotation of $0.24 \pm 0.07^\circ$ for 1 mm of

translational excursion. Fig. 4 shows two observation periods for a single sample case with a pronounced connection of pitch and anterior/posterior motion. Roll and yaw rotations changed independently for all cases, with no correlation with translational shifts.

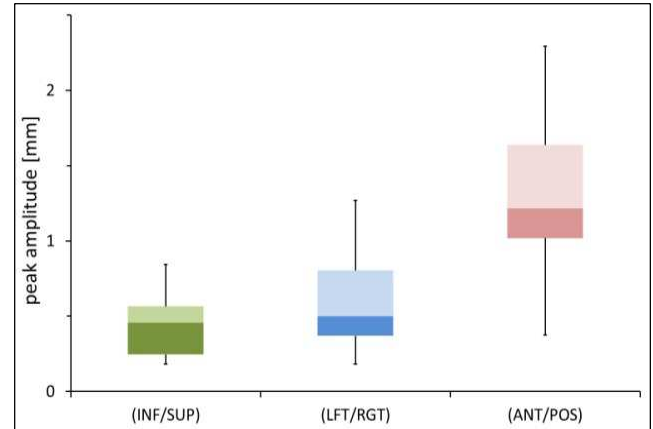


Figure 3. Box-whisker-plots of peak amplitude A for stochastic motion in the three translational degrees of freedom.

The median drift over 10 minutes was 0.29 mm along the inferior/superior, 0.57 mm along the left/right and 0.64 mm along the anterior/posterior axis (fig. 5). The median total translational drift (RMS) was 1.08 mm. Only for two patients, a total drift of more than 3 mm was encountered over the 10 minute timeframe (fig. 5).

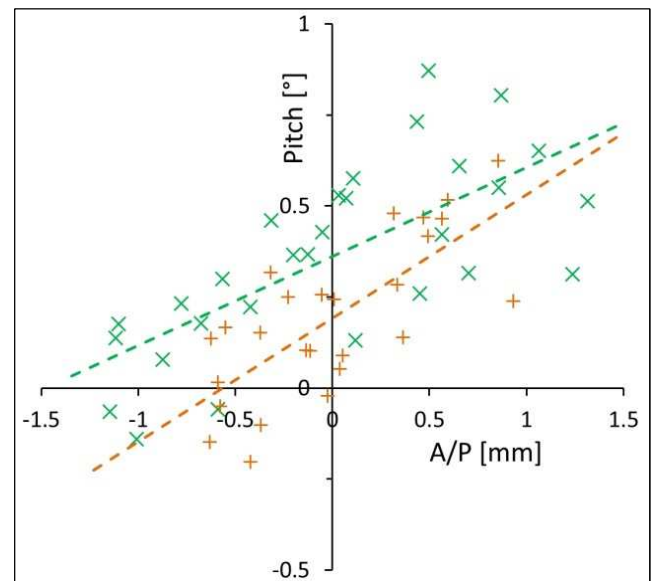


Figure 4. Anterior/posterior (A/P) motion vs. pitch. Two observations periods (11.2 and 14.8 minutes) of a sample case are given. A linear correlation (Pearson's coefficient $r = 0.71$ for the turquoise and 0.74 for the brown plot) was observed. On average, 1 mm anterior/posterior motion corresponded to a spine tilt of 0.29° for this patient.

DISCUSSION

We adopted a prone setup technique intended to stabilize the target spine region. The applied immobilization measures were found to allow for small drifts in position during treatment. Hoogeman et al. (11) reported a mean drift (RMS) of 1.2 mm over 15 minutes for extracranial supine treatments and 2.2 mm for prone position, respectively. In comparison, our data lies almost exactly in the middle of these two values, which is evidence that our patient setup is adequately stable.

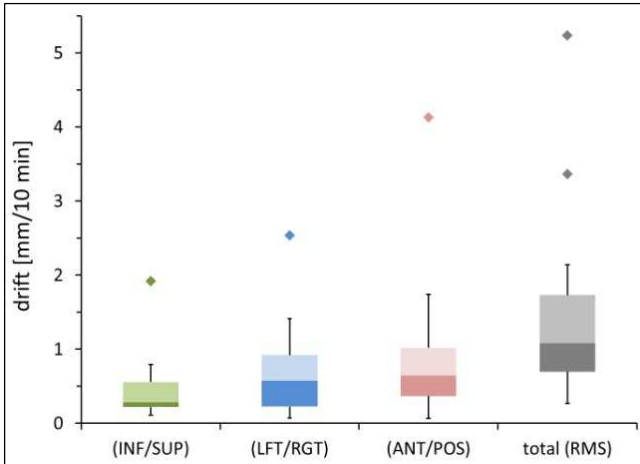


Figure 5. Box-whisker-plots of the translational drift per 10 minutes. Outliers are indicated.

In terms of the stochastic component, prone patient position resulted in substantial amount of motion in anterior/posterior direction, which significantly exceeded movement along the left/right ($p=7.4 \times 10^{-5}$, paired student t-test) and superior/inferior ($p=9.1 \times 10^{-7}$, paired student t-test) axes. The pronounced correlation with spine pitch is indication that the anterior/posterior motion of the lumbar/sacral spine was not of a strictly “stochastic” nature, but was mainly induced by movement of the abdomen and/or chest due to breathing.

Even though the tracking region of interest was always centered on the same vertebrae, the extent and characteristics of observed motion patterns during treatment were very diverse. Furthermore, we experienced one case of a patient who could not be adequately stabilized already during CT scanning, despite our best efforts. Therefore, this patient was not selected for treatment in prone position. In our experience, the individual patient anatomy is the key factor that determines whether prone treatment is advisable, and which immobilization measures are most successful. In particular, obese patients with a large abdominal girth are difficult to stabilize. Close monitoring and refining of setup procedures by expert personnel is crucial for patient safety.

Finally, we want to deduce a suitable PTV margin to account for the additional uncertainty. In a DVH-based approach, van Herk et al. (13) have derived a simple formula for calculation of margins. They distinguish between “preparation” errors causing a systematic shift and stochastic “execution” errors causing a blurring of the dose distribution. For a multiple fraction treatment, a standard CTV-to-PTV margin m_{PTV} can then be approximated by

$$m_{PTV} = 2.5\Sigma + 0.7\sigma \quad (2)$$

which corresponds to 95% coverage for 90% of the patients and a width of 3.2 mm for the penumbra. Σ and σ refer to the standard deviations of preparation and execution errors (13).

This recipe has been derived assuming multiple fractions, where the average of the random error over the whole treatment course is zero. This assumption is not fulfilled for single-fraction CK treatments, and therefore, eq. [2] is not directly applicable. However, Hoogeman et al. (11) have adopted the formalism to estimate a margin applicable to single fraction, image-guided treatments by using the standard deviation of the intrafraction drift as the systematic error Σ and the standard deviation of the stochastic motion component as σ . We followed their approach and used our drift and stochastic motion data as input parameters. Based on the average frequency of 1.4 stereoscopic image acquisitions per minute for our observation periods, we assumed a longer imaging interval of 1 minute as a conservative estimate. With these values, we calculated a value of 0.10 mm for Σ . A value of 1.58 mm was determined for σ , assuming sinusoidal stochastic motion with the measured peak amplitudes A . Using eq. [2], m_{PTV} amounts to 1.4 mm.

Up to this point, the impact of rotations as a potential source of error has been neglected in the calculation of m_{PTV} (13). Respiration-induced pitch motion and residual stochastic rotations add to the uncertainty. A distance of up to 6 cm between the center of the tracking ROI and the lesion, which is representative for lumbar/sacral targets, and a conservative estimate of 1 degree for the rotational error correspond to an additional targeting error of up to 1 mm on top of the value calculated with translations only.

We therefore recommend and have chosen to apply a uniform margin of 3 mm to assure adequate target coverage.

In comparison, CK spinal treatments in supine position can be performed with submillimeter accuracy (9), with no need for an additional margin. Since, effectively, a larger target must be treated in prone position, this countervails a potential dosimetric advantage due to shorter beam paths. Furthermore, a new optimized supine setup technique using a thick foam pad improves lateral access with the CK (14), which can also be beneficial for posterior lesions in the lumbar/sacral spine. In order to develop clear patient selection criteria for prone treatment in the future, a comparative planning study is needed. This study must include different margins to correctly account for target motion.

CONCLUSIONS

We have demonstrated the feasibility of fiducial-free prone treatments in the lower lumbar and sacral spine, thus further extending the usability of the CyberKnife. When suitable immobilization techniques are applied, the target motion due to breathing can be limited to a few millimeters overall. This can be compensated by a slightly increased size of the PTV, which must be carefully weighed against a presumed dosimetric benefit due to posterior radiation access.

REFERENCES

1. Hsu W, Nguyen T, Kleinberg L, Ford EC, Rigamonti D, Gokaslan ZL, Lim M. Stereotactic radiosurgery for spine tumors: review of current literature. *Stereotact Funct Neurosurg*. 2010;88(5):315-21. Epub 2010 Aug 13.
2. Gerszten PC, Burton SA. Clinical assessment of stereotactic IGRT: spinal radiosurgery. *Med Dosim* 2008;33:107-116.
3. Agazaryan N, Tenn SE, Desalles AA, Selch MT. Image-guided radiosurgery for spinal tumors: methods, accuracy and patient intrafraction motion. *Phys Med Biol* 2008;53:1715-1727.

4. Chang Z, Wang Z, Ma J, O'Daniel JC, Kirkpatrick J, Yin FF. 6D image guidance for spinal non-invasive stereotactic body radiation therapy: Comparison between ExacTrac X-ray 6D with kilo-voltage cone-beam CT. *Radiother Oncol.* 2010 Apr;95(1):116-21. Epub 2010 Feb 1.
5. Muacevic A, Staehler M, Drexler C, Wowra B, Reiser M, Tonn JC. Technical description, phantom accuracy, and clinical feasibility for fiducial-free frameless real-time image-guided spinal radiosurgery. *J Neurosurg Spine* 2006;5:303-312.
6. Kilby W, Dooley JR, Kuduvalli G, Sayeh S, Maurer CR Jr. The CyberKnife Robotic Radiosurgery System in 2010. *Technol Cancer Res Treat.* 2010 Oct;9(5):433-52.
7. Accuray Inc., Sunnyvale, CA, USA. *Treatment Delivery Manual, CyberKnife version 8.5.x.* 2009.
8. Ho AK, Fu D, Cotrutz C, Hancock SL, Chang SD, Gibbs IC, Maurer CR, Adler JR. A study of the accuracy of Cyberknife spinal radiosurgery using skeletal structure tracking. *Neurosurgery* 2007;60:147-156.
9. Fürweger C, Drexler C, Kufeld M, Muacevic A, Wowra B, Schlaefer A. Patient Motion and Targeting Accuracy in Robotic Spinal Radiosurgery: 260 Single-Fraction Fiducial-Free Cases. *Int J Radiat Oncol Biol Phys.* 2010 Nov 1;78(3):937-45. Epub 2010 Apr 13.
10. Muacevic A, Drexler C, Kufeld M, Romanelli P, Duerr HJ, Wowra B. Fiducial-free real-time image-guided robotic radiosurgery for tumors of the sacrum/pelvis. *Radiother Oncol.* 2009 Oct;93(1):37-44. Epub 2009 Jun 22.
11. Hoogeman MS, Nuyttens JJ, Levendag PC, Heijmen BJM. Time dependence of intrafraction patient motion assessed by repeat stereoscopic imaging. *Int J Radiat Oncol Biol Phys* 2008;70:609-618.
12. Ma L, Sahgal A, Hossain S, Chuang C, Descovich M, Huang K, Gottschalk A, Larson DA. Nonrandom intrafraction target motions and general strategy for correction of spine stereotactic body radiotherapy. *Int J Radiat Oncol Biol Phys.* 2009 Nov 15;75(4):1261-5. Epub 2009 Aug 3.
13. Van Herk M, Remeijer P, Lebesque JV. Inclusion of geometric uncertainties in treatment plan evaluation. *Int J Radiat Oncol Biol Phys.* 2002 Apr 1;52(5):1407-22.
14. Hevezi JM. A new patient support pad for CyberKnife planning & delivery - a technical note. <http://www.peeremed.com>. Epub 2010 Oct 28.